Dual Cluster Contrastive learning for Person Re-Identification

Hantao Yao, Changsheng Xu
National Laboratory of Pattern Recognition, Institute of Automation, CAS
hantao.yao@nlpr.ia.ac.cn

Abstract

Recently, cluster contrastive learning has been proven effective for person ReID by computing the contrastive loss between the individual feature and the cluster memory. However, existing methods that use the individual feature to momentum update the cluster memory are not robust to the noisy samples, such as the samples with wrong annotated labels or the pseudo-labels. Unlike the individual-based updating mechanism, the centroid-based updating mechanism that applies the mean feature of each cluster to update the cluster memory is robust against minority noisy samples. Therefore, we formulate the individual-based updating and centroid-based updating mechanisms in a unified cluster contrastive framework, named Dual Cluster Contrastive learning (DCC), which maintains two types of memory banks: individual and centroid cluster memory banks. Significantly, the individual cluster memory is momentum updated based on the individual feature. The centroid cluster memory applies the mean feature of each cluter to update the corresponding cluster memory. Besides the vallina contrastive loss for each memory, a consistency constraint is applied to guarantee the consistency of the output of two memories. Note that DCC can be easily applied for unsupervised or supervised person ReID by using ground-truth labels or pseudo-labels generated with clustering method, respectively. Extensive experiments on two benchmarks under ***supervised person ReID*** *and* ***unsupervised person ReID*** *demonstrate the superior of the proposed DCC. Code is available at: https://github.com/htyao89/Dual-Cluster-Contrastive/*

1. Introduction

Person Re-identification (ReID) aims to search the probe person from different camera-views, attracting increasing attention because of the growing demands in practical video surveillance. Based on whether using the human annotated labels, person ReID can be divided into supervised person ReID and unsupervised person ReID. The supervised person ReID aims to infer a discriminative person description with the annotated labels [2,5,9,23,44,50,52,60]. Since collecting the massive identity annotations is time-consuming and expensive, unsupervised person ReID infers the person description with the pseudo-labels [11, 16, 17, 32, 49, 57], *e.g.,* the pseudo-labels inferred by clustering methods from the unlabeled data are used for unsupervised person ReID.

Recently, contrastive learning has been widely exploited for unsupervised representation learning [1, 8, 10, 18], aiming to learn the invariance feature with a self-supervised mechanism based on sample self-augmented. Inspired by vallina contrastive learning, cluster contrastive learning has received more attention for person ReID [13, 18, 30, 45]. The cluster contrastive learning in person ReID builds a cluster-level memory dictionary in which a single feature vector represents each cluster [13], shown in Figure 1(a). For example, Dai *et al.* [13] store the feature vectors and compute contrast loss in the cluster level, and Li *et al.* [30] propose an asymmetric contrastive learning framework to exploit both the cluster structure and the individual feature to conduct effective contrastive learning for person ReID. However, previous methods apply the individual feature to update the cluster memory. The cluster contrastive with individual-based updating mechanism is not robust to the noisy samples, *e.g.,* the samples with wrong annotated labels or the pseudo-labels.

To address the above problem, we consider dual complementary memory updating mechanisms for the cluster contrast. Besides the individual-based update mechanism of the vanilla cluster contrastive, we also introduce a novel centroid-based update mechanism to reduce the influence of noisy samples, *e.g.,* the samples with wrong annotated labels or the pseudo labels. Unlike the individual-based updating mechanism that uses the individual feature to update the corresponding visual term of the cluster memory, the centroid-based update mechanism applies the mean feature of each cluster or class to update the corresponding cluster memory, shown in Figure 1(b). Although the provided labels might contain some incorrect labels, most of them are correct, thus using the mean feature to represent each group can reduce the influence of the incorrect features. From the perspective of optimization, the individual-based updating

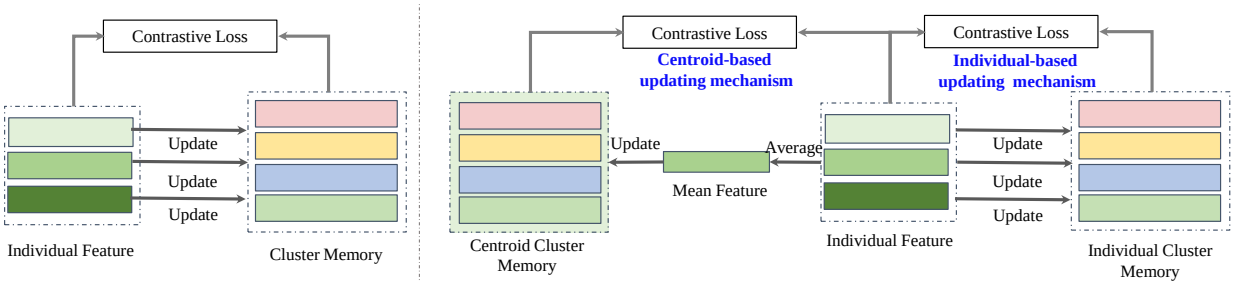

Figure 1. Comparison with the Vallina Cluster Contrastive learning (a), and the proposed Dual Cluster Contrastive Learning (b). Feature vectors in different shades of green are of the same identity.

mechanism can be treated as the Stochastic Gradient Descent, which considers just one individual at a time to take a single step for updating the parameters. However, considering just an individual sample will fluctuate over the training examples, especially for the noisy samples. The centroid-based updating mechanism is similar to the Batch Gradient Descent, which is proposed to reduce the impact of individual samples by considering all training data in a single step, *e.g.,* it takes the average of the gradients of all the training examples and then uses the mean gradient to update our parameters. Furthermore, the individual-based update mechanism constructs the embedding space based on considering all individual samples, and the centroid-based updating mechanism aims to generate a stable embedding space by considering the mean description of each cluster. Therefore, the cluster contrastive learningwith the centroid-based updating mechanism can complement the individual-based updating mechanism. Consequently, considering those two updating mechanisms, the dual cluster contrastive learning can improve the stability and discriminatory of features.

Based on the above motivation, we propose a novel Dual Cluster Contrastive (DCC) framework in which an Individual Cluster Memory bank and a Centroid Cluster Memory bank are employed to implement the individual-based and centroid-based updating mechanism, as shown in Figure 2. The Individual Cluster Memory bank uses the individual features and their labels to update the corresponding cluster memory. Meanwhile, the Centroid Cluster Memory bank applies the average of features belonging to the same cluster for momentum updating. Especially, using the Individual Cluster Memory and Centroid Cluster Memory can embed the instance's features into the individual-level prediction and centroid-level prediction, respectively. Besides the standard contrastive loss for each memory bank, a consistency constraint is applied to guarantee the consistency of the two types of predictions. In the inference stage, the backbone is used to extract the query and gallery features for retrieval. The DCC can be easily applied for unsupervised or supervised person ReID by using ground-truth labels or pseudo-labels generated with clustering method, respectively.

In summary, to overcome the limitation of the vanilla cluster contrastive learning, we propose a novel Dual Cluster Contrastive learning framework for person ReID, consisting of the individual-level and centroid-level cluster contrast. The evaluation on two benchmarks under supervised and unsupervised person ReID settings show the effectiveness of the DCC. 1) **supervised person ReID**: DCC obtains the mAP of 89.8%, and 64.9% for Market-1501, and MSMT17, respectively. 2) **unsupervised person ReID**: DCC obtains the mAP of 84.7%, and 41.8% for Market-1501, and MSMT17, respectively. The experiment also shows that DCC has the advantages of fast training convergence, insensitivity to batch size, and high generalization.

2. Related Work

In this section, we give a brief review of the supervised person ReID and the unsupervised person ReID.

2.1. Supervised Person Re-identification

Based on manually annotated labels, many methods have been proposed for supervised person ReID and achieved promising performance. Some methods focus on CNN structure designing for feature extraction. For example, Zheng *et al.* [53] and Fu *et al.* [16] extract local features from several horizonal stripes to explore the discriminative clues. Several work use human pose estimation [29] or human semantic parsing [27] to extract local features. Furthermore, many novel attention modules have been proposed for supervised person ReID [2, 5, 44, 50, 52]. Recently, inspired by the success of transformer structure, He *et al.* [21] and Lai *et al.* [28] adopt transformer structure to explore the discriminative clues for supervised person ReID.

There are also some researchers studying on metric learning [9, 23, 60, 61]. For example, Hermans *et al.* [23] apply triplet loss on person ReID and largely boost the performance. Several researchers try to enhance the training efficiency of triplet loss, *e.g.*, Chen *et al.* [9] introduce an extra negative sample in triplet loss to form the quadruplet for

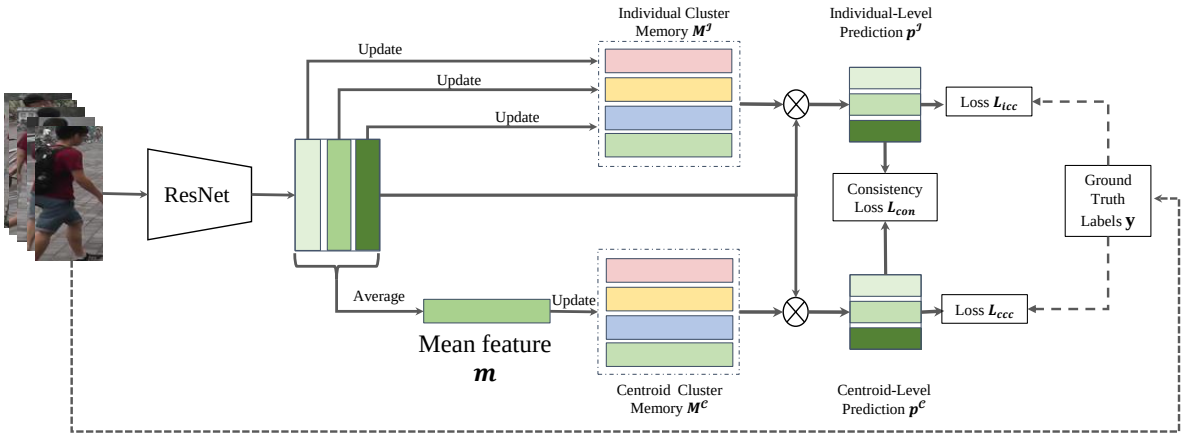

Figure 2. The framework of proposed Dual Cluster Contrastive learning for supervised person ReID. Given the training images, we apply the backbone to extract the feature. Then, Individual Cluster Memory and Centroid Cluster Memory are used to represent two types of cluster centers. The Centroid Cluster Memory uses the mean feature of each cluster for update. Feature vectors in different shades of green are of the same identity.

model training. Additionally, Wojke *et al.* [41] apply cosine softmax classifier proposed on supervised person ReID.

2.2. Unsupervised Person Re-identification

As manual annotations are expensive and unavailable in real-world applications, unsupervised person ReID has attracted much more attention. Some researchers use extra labeled images to assist the unsupervised training on unlabeled person ReID by transferring labeled images to the unlabeled domains with GAN-based models [11, 32, 40, 57] or narrowing the distribution gap in feature space [12, 24, 33]. For example, Liu *et al.* [32] use three GAN models to reduce the discrepancy between different domains in illumination, resolution, and camera-view, respectively. To handle the lack of annotation, many methods have been proposed to acquire reliable pseudo labels [15, 31, 46, 47, 54]. For example, Lin *et al.* [31] propose a bottom-up unsupervised clustering method that simultaneously considers both diversity and similarity.

Given pseudo labels, some methods use triplet loss for model training [16, 17, 48, 49]. As triplet loss only optimizes distance relationship between selected samples in training batches, several methods further adopt memory bank and contrastive loss to involve more sample distance relationships in training [3, 4, 13, 18, 26, 30, 45, 58]. For example, Zhong *et al.* [58] save features of all the images in the unlabeled training set in the memory bank for contrastive learning, Chen *et al.* [3] save a proxy feature for each class in the memory bank, and Ge *et al.* [18] propose a hybrid memory bank that saves both instance features and class proxy. Dai *et al.* [13] present the Cluster Contrast mechanism, which stores feature vectors and computes contrast loss in cluster level memory dictionary. Li *et al.* [30] propose an asymmetric contrastive learning framework to exploit both the cluster structure and the invariance in augmented data to conduct effective contrastive learning for person ReID.

However, these methods update the memory bank with every single feature in training batches, making features in memory easily affected by noisy samples. Compared with previous methods, DCC additionally introduces a centroid updated memory bank that updates based on class mean features of each cluster in training batches. As mean features are robust against minority noisy samples, updating the memory bank with class centroids will enhance the robustness of the memory bank against label noise and improve the training efficiency and the ReID performance. Experiments also show that DCC has the advantages of fast training convergence, insensitivity to batch size, and high generalization.

3. Methodology

Given a training dataset $D = \{(x_i, y_i)\}_{i=1}^{N}$, the person re-identification (ReID) aims to learn a robustness backbone Φ for person retrieval, where x_i and $y_i \in [1, N_c]$ denotes the i-th training image and its label, respectively. N is the number of the training images, and N_c denotes the number of identities. For convenience, we use $\mathbf{X}$ and $\mathbf{Y}$ to represent the set of training images and labels. Actually, the supervised and unsupervised person ReID can be formulated with the same unified framework once providing the annotated labels or generating the pseudo-labels. For the supervised person ReID, the ground-truth $\mathbf{Y}$ is annotated by the human. For the unsupervised person ReID, the pseudo-labels $\hat{\mathbf{Y}}$ can be generated with a clustering algorithm. For convenience, we denote $\mathbf{Y}$ as the obtained annotations for both supervised and unsupervised person ReID tasks to describe the proposed methodology.

3.1. Cluster Contrastive

With the above definition, we firstly give a review of the vallina cluster contrastive. It contains two components: Backbone Φ, and Cluster Memory Bank $\mathbf{M}$, in which each cluster is represented by a mean feature and all cluster feature vectors are consequently updated based on individual feature, as shown in Figure 1(a). Given all training images $\mathbf{X}$, the backbone Φ is used to extract the corresponding features $\mathbf{F} = \Phi(\mathbf{X})$. Then, Cluster Memory bank $\mathbf{M} \in \mathbb{R}^{N_c \times N_d}$ is initialized with the mean feature of each class, where N_d and N_c are the feature dimension and number of classes, respectively. Based on the pretrained feature $\mathbf{F}$, the visual center $\mathbf{M}_j$ of the j-th class is initialized with Eq. (1),

$$\mathbf{M}_j = \frac{1}{\mathcal{N}(\mathbf{F}_j)} \sum_{\mathbf{f} \in \mathbf{F}_j} \mathbf{f}, \tag{1}$$

where $\mathbf{F}_j$ denotes the feature set of images belonging to the j-th class, $\mathcal{N}(\mathbf{F}_j)$ represents the number of features in set $\mathbf{F}_j$, $\mathbf{f} \in \mathbb{R}^{1 \times N_d}$ is an image feature, and $\mathbf{M}_j$ denotes the j-th cluster feature in Cluster Memory Bank $\mathbf{M}$.

Since Cluster Memory bank $\mathbf{M}$ can be treated as a non-parametric classifier, it can produce the class prediction used for contrastive loss, formulated as Eq. (2),

$$\mathcal{L} = -log \frac{exp(\mathbf{f}_i \cdot \mathbf{M}_{y_i})/\tau}{\sum_{j=1}^{N_c} exp(\mathbf{f}_i \cdot \mathbf{M}_j)/\tau}, \tag{2}$$

where τ is a temperature hyper-parameter [43], and y_i is the corresponding label for the image feature $\mathbf{f}_i$. When the feature $\mathbf{f}_i$ has a higher similarity to its ground-truth visual centers $\mathbf{M}_{y_i}$ and dissimilarity to all other cluster features, the objective loss $\mathcal{L}$ has a lower value.

In vanilla cluster contrastive learning, the individual feature is applied to momentum update the Cluster Memory bank $\mathbf{M}$ during forward propagation with Eq. (3),

$$\mathbf{M}_{y_i} = \omega \mathbf{M}_{y_i} + (1 - \omega) \cdot \mathbf{f}_i, \tag{3}$$

where $\mathbf{f}_i$ and y_i is the feature and label for image x_i, respectively. $\mathbf{M}_{y_i}$ is the y_i-th cluster feature in Cluster Memory Bank $\mathbf{M}$.

Although the cluster contrastive learning can generate the discriminative descriptions, it is not robust to the noisy samples[1], especially for the unsupervised person ReID that relies heavily on the accuracy of the pseudo labels. The main reason is that the updating policy of the memory bank with Eq. (3) is based on the individual feature, including the noisy samples. Specifically, ω is usually set to a lower value for the cluster contrastive learning, *e.g.,* ω=0.1 in [13]. From Eq. (3), we can observe that the mean feature in the cluster memory $\mathbf{M}$ is severely affected by the individual feature. Therefore, the noisy samples might have a serious negative impact. An intutive illustration is shown in Figure 3.

[1]The noisy samples denotes the sample with incorrect labels

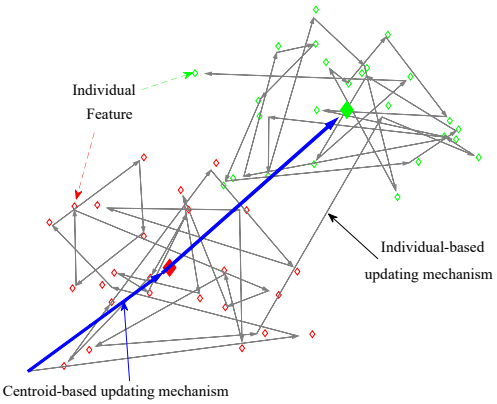

Figure 3. The update process of the Individual-based (Grey arrow line) and Centroid-based updating mechanism (Blue arrow line). Individual-based updating mechanism is easily affected by individual feature, especially outlier samples. ◇ and ◇ denote the individual feature belonging to the same class from different batches, respectively. ♦ and ♦ are the corresponding center features.

3.2. Dual Cluster Contrastive

To overcome the limitation of the vallina cluster contrastive, we propose a novel Dual Cluster Contrastive (DCC) framework, as shown in Figure 2. The significant difference between the Dual Cluster Contrastive and the vallina cluster contrastive is that DCC maintains two types of memory banks to model the feature distribution from two perspectives, *i.e.,* Individual Cluster Memory bank and centroid Cluster Memory bank. Similar to the vallina cluster contrastive, the individual memory bank is updated based on each individual. Besides, the centroid cluster memory is used to model the class distribution based on the mean feature of each class, which is robust against minority noisy samples.

In Dual Cluster Contrastive, the individual cluster memory and the centroid cluster memory are defined as $\mathbf{M}^{\mathcal{I}}$ and $\mathbf{M}^{\mathcal{C}}$, respectively. Note that $\mathbf{M}^{\mathcal{I}}$ and $\mathbf{M}^{\mathcal{C}}$ are both initialized based on the mean pretrained feature of each cluster with Eq. (1). Given the feature $\mathbf{f}_i$ along with its label y_i, the memory bank $\mathbf{M}^{\mathcal{I}}$ is momentum updated with Eq. (4),

$$\mathbf{M}^{\mathcal{I}}_{y_i} = \omega \mathbf{M}^{\mathcal{I}}_{y_i} + (1 - \omega) \cdot \mathbf{f}_i. \tag{4}$$

For the centroid cluster memory, we apply the mean feature of each class for momentum updating. Specifically, we first compute each class's mean feature during training and then update the centroid cluster memory with the obtained mean feature. Therefore, the cluster memory $\mathbf{M}^{\mathcal{C}}$ is updated with Eq (5),

$$\mathbf{M}^{\mathcal{C}}_{y_i} = \omega \mathbf{M}^{\mathcal{C}}_{y_i} + (1 - \omega) \cdot \mathbf{m}_{y_i}, \tag{5}$$

Algorithm 1 The procedure of DCC

Require: Given the dataset $D = \{(x_i, y_i)\}_{i=1}^{N}$
Require: Initialize the backbone Φ with ResNet-50 pretrained on the ImageNet.
Require: Initialize the individual cluster memory $\mathbf{M}^{\mathcal{I}}$ and centroid cluster memory $\mathbf{M}^{\mathcal{C}}$ with the mean feature of each cluster.

```
while epoch≤ total_epoch do
    Sample training images X from D;
    Extracting the corresponding features F with backbone Φ(X);
    Computing the classification and consistency losses based on features F and the memories M^I and M^C with Eq. (10);
    Updating the individual cluster memory M^I with Eq. (4);
    Updating the centroid cluster memory M^C with Eq. (5);
end while
```

Output: The trained model Φ.

where $\mathbf{m}_{y_i}$ denotes the mean feature of the y_i-th class in each mini-batch, which is caluated as follows:

$$\mathbf{m}_{y_i} = \frac{1}{\mathcal{N}(\mathbf{F}_{y_i})} \sum_{\mathbf{f} \in \mathbf{F}_{y_i}} \mathbf{f}, \tag{6}$$

where $\mathbf{F}_{y_i}$ denotes the set of features belonging to the y_i-th class, $\mathcal{N}(\mathbf{F}_{y_i})$ represents the number of features in set $\mathbf{F}_{y_i}$, $\mathbf{f}$ is an instance feature. L2-normalization is used to normalize the $\mathbf{m}_{y_i}$.

During training, given the image x along with its feature $\mathbf{f}$, using the cluster memories $\mathbf{M}^{\mathcal{I}}$ and $\mathbf{M}^{\mathcal{C}}$ can generate the two types of predictions $\mathbf{p}^{\mathcal{I}} = \mathbf{f}(\mathbf{M}^{\mathcal{I}})^{\top}$ and $\mathbf{p}^{\mathcal{C}} = \mathbf{f}(\mathbf{M}^{\mathcal{C}})^{\top}$. To boost the representation learning, the consistency loss is applied to constrain the consistency of those two predictions,

$$\mathcal{L}_{con}(\mathbf{f}) = H(\mathbf{p}^{\mathcal{I}}, \mathbf{p}^{\mathcal{C}}), \tag{7}$$

where $H(\cdot)$ is smooth L1 loss for measuring the distance between two predictions.

Besides the consistency loss, the contrastive loss is also conducted for individual-level and centroid-level cluster contrastive, *e.g.,* the centroid-level cluster contrastive loss $\mathcal{L}_{ccc}$ and the individual-level cluster contrastive loss $\mathcal{L}_{icc}$ for the feature $\mathbf{f}$ are computed as follows:

$$\mathcal{L}_{ccc}(\mathbf{f}) = -log\frac{exp(\mathbf{f} \cdot \mathbf{M}_y^{\mathcal{C}})/\tau}{\sum_{j=1}^{N_c} exp(\mathbf{f} \cdot \mathbf{M}_j^{\mathcal{C}})/\tau}, \tag{8}$$

$$\mathcal{L}_{icc}(\mathbf{f}) = -log\frac{exp(\mathbf{f} \cdot \mathbf{M}_y^{\mathcal{I}})/\tau}{\sum_{j=1}^{N_c} exp(\mathbf{f} \cdot \mathbf{M}_j^{\mathcal{I}})/\tau}, \tag{9}$$

where y is the class label for the feature $\mathbf{f}$.

Therefore, the final loss is:

$$\mathcal{L}_{dcc} = \mathcal{L}_{ccc} + \mathcal{L}_{icc} + \lambda\mathcal{L}_{con}, \tag{10}$$

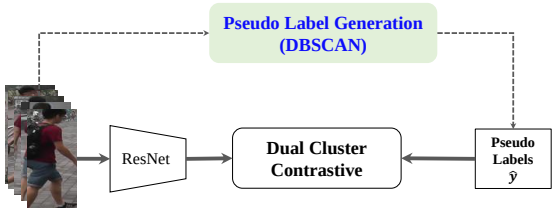

Figure 4. The framework of proposed Dual Cluster Contrastive learning for unsupervised person ReID.

where λ is a weight to balance the effect of the classification loss and consistency loss. The algorithm is illustrated in Algorithm 1.

3.3. Generalize to unsupervised person ReID

Existing unsupervised person ReID commonly uses the clustering methods to generate the pseudo-labels for unlabeled images, and then perform supervised training based on the generated pseudo-labels. With the pseudo-labels, the proposed Dual Cluster Contrastive can be easily applied for unsupervised person ReID.

Specifically, given the unlabeled training images, we firstly apply the backbone to extract the corresponding features. Similar to [13], we apply DBSCAN to group all training features into several groups. Then, the cluster ID is assigned to each training image as the pseudo-label, and the unclustered outlier images are discarded from training. With the pseudo-labels, the proposed Dual Cluster Contrastive is conducted for representation learning, shown in Figure 4.

4. Experiments

4.1. Datasets

We conduct experiments on two benchmarks under the supervised and unsupervised settings to evaluate the effectiveness of the proposed Dual Cluster Contrastive .

Market-1501 [55] contains 32,668 images of 1,501 identities captured from six camera-views. The 12,936 images belonging to 751 identities are the training images, and the resting 19,732 images of 750 identities are used for testing.

MSMT17 [40], which is a challenger and larger dataset than Market1501, contains a total of 126,441 images under 15 camera-views. In the training set, there are 1,041 identities with 32,621 images. In the testing set, there are 93,820 images of 3,060 identities.

4.2. Implementation Details

The proposed Dual Cluster Contrastive is implemented based on the existing cluster contrastive framework [13][2]. We adopt the ResNet-50 [19] pretrained on ImageNet [14]

[2]https://github.com/alibaba/cluster-contrast-reid

BatchSize	64	80	96	128	160	192
CCC	87	87.6	88	87.1	86.5	86.1
ICC	82.9	85.4	87.7	88.5	88.8	88.6
DCC	**87.3**	**88**	**89**	**89.2**	**88.8**	**88.6**

Table 1. Effect of proposed component in Dual Cluster Contrastive on Market-1501(mAP(%)).

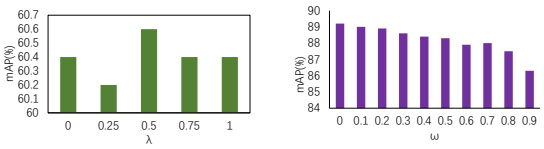

(a) λ (b) ω

Figure 5. The effect of λ and ω for DCC.

as the backbone. Inspired by [34], all sub-module layers after layer4-1 are removed, and a GEM pooling followed by batch normalization layer [25] and L2-normalization layer is added. Therefore, the feature dimension N_d is 2,048. The adam optimizer with a weight decay of 0.0005 is used to train the network in 150 epochs. The learning rate is initially set as 0.00035 and decreased to one-tenth of every 50 epochs. The temperature coefficient τ is set to 0.05. All input images are resized 256×128 for training. Inspired by [13], for the unsupervised person ReID, DBSCAN is used to generate pseudo labels for the Dual Cluster Contrastive. We sample P person identities and a fixed number K instances for each person identity during training. Therefore, the batch size is $P \times K$. In this work, we set K=16, and change P for adjusting the batch size. Finally, P is set as 16, and the batch size is 128. During testing, we apply the inferred backbone to extract features, and then apply the Euclidean distance for retrieval.

4.3. Ablation Studies

In this section, we conduct some ablation studies on Market1501 and MSMT17 to evaluate the effectiveness of the proposed component in Dual Cluster Contrastive.

Effect of Dual Cluster Contrastive As mentioned above, Dual Cluster Contrastive(DCC) consists of the Individual-level Cluster Contrastive(ICC) and Centroid-level Cluster Contrastive(CCC), where CCC is the significant contribution module from existing methods. Therefore, we analyze the effectiveness of the Centroid-level Cluster Contrastive and Dual Cluster Contrastive, and summarize the results in Table 1. We observe that the ICC model obtains a higher performance than the CCC model, *e.g.,* ICC obtains the best mAP of 88.8% by setting the batch size as 160. However, the Centroid-level Cluster Contrastive is more effective to the smaller batch size, *e.g.,* CCC obtains a higher performance than ICC for the batch size from 64 to 96. Furthermore, DCC combining two types of cluster contrastive learning obtains the best performance

Methods	Market-1501		MSMT17	
	mAP	R1	mAP	R1
All	89.2	95.4	60.6	82.5
Random	88.9	95.1	60.6	82.4
Hard	89.2	95.8	60.4	82.0

Table 2. Effect of different update polices.

on all batch sizes, proving that the Centroid-level Cluster Contrastive complements the Individual-level Cluster Contrastive. Therefore, Dual Cluster Contrastive is a reasonable framework for cluster contrastive. From Table 1, we also observe that DCC is insensitive to changes of batch size. For example, the ICC model obtains the mAP of 88.5% for the batch size of 160. However, once reducing the batch size to 64, its mAP quickly plummets to 82.9%. Differently, DCC obtains the mAP 88.8% and 87.3% for the batch size of 160 and 64, respectively.

Effect of Consistency Loss The consistency loss constrains two types of memories to produce the predictions for the given images. In Eq (10), λ is a hyper-parameter to balance the effect of the consistency loss. We thus analyze the effect of λ and summarize the results in Figure 5a. It can be observed that setting the lower and higher λ both achieve the worse performance, *e.g.,* setting λ=0.5 obtains the mAP of 60.6%, which is higher than 60.4% for λ=0.0 and λ=1.0, respectively.

Effect of different updating polices for Individual Cluster Memory There exist three types of updating policies for the individual cluster memory, *i.e.,* "Random", "All", and "Hard". "Hard" means the individual-level cluster contrastive uses the most dissimilar samples of each class to update the memory bank. "Random" and "All" mean that we use all samples and randomly select a sample of each class for updating, respectively. As shown in Table 2, "All" strategies obtains the best performance, *e.g.,* obtaining the mAP of 89.2% and 60.6% for Market-1501 and MSMT17, respectively.

Effect of momentum value ω Similar to existing contrastive learning, the momentum updating strategies is applied to update cluster features in individual-level and centroid-level memory cluster memory banks. Note that the individual-level and centroid-level cluster memory banks use the same momentum value ω. We thus analyze the effect of momentum value ω. As shown in Figure 5b, the smaller ω performs better than higher ω, *e.g.,* ω=0.0 obtains the highest performance. Therefore, we set ω=0.0 in this work.

Effect of Batch Size To evaluate the impact of batch size on Dual Cluster Contrastive, we compare the batch size from 64 to 192. As shown in Table 1, increasing the batch size would first increase and then decrease performance, *e.g.,* using the batch size of 128 obtains the highest mAP of 89.2%, which is higher than the batch size of 64 and

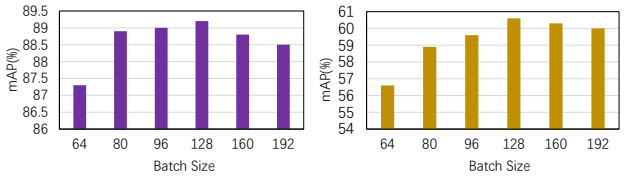

(a) Market1501 (b) MSMT17

Figure 6. The effect of batch size on Market1501 and MSMT17.

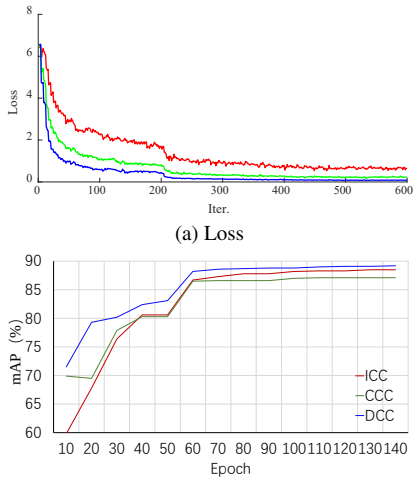

(a) Loss

(b) mAP

Figure 7. The change of loss and mAP during training on Market1501.

192. Figure 6 further gives the performance of different batch sizes on the Market-1501 and MSMT17 datasets for the proposed DCC.

Training Convergence We further analyze the training convergence process of DCC. Figure 7a summarizes the training loss of different models, *e.g.,* individual-level, centroid-level, and dual cluster contrastive models. Furthermore, we summarize the change in mAP of different models in Figure 7b. We can observe that the dual cluster contrastive achieves a lower loss and a higher performance with a faster convergence speed. For example, Dual Cluster Contrastive obtains the mAP of 88.5% for the 60-th epoch, which is higher than the performance for the individual-level and centroid-level cluster contrastive.

4.4. Comparison with existing methods

In this section, we conduct the comparison with existing methods following two settings: *supervised person ReID*, and *unsupervised person ReID*.

Comparision on Supervised Person ReID We first compare the Dual Cluster Contrastive with existing supervised person ReID methods on two benchmarks and summarize the results in Table 3, and Table 4 for Market1501, and MSMT17, respectively. We perform the comparison from three aspects to prove the effectiveness of the proposed DCC.

Methods	mAP	R1	R5	R10
CAR [59]	84.9	94.8	-	-
SCAL [2]	85.0	95.1	98.1	98.9
MGN [39]	86.9	95.7	-	98.93
CAL [36]	87.0	94.5	97.9	-
Cluster Contractive [13]	87.0	94.6	98.2	98.8
Circle Loss [37]	87.4	**96.1**	-	-
CLA [6]	88.0	95.4	-	-
FastReID(ResNet50) [20]	88.2	95.4	-	-
RGA-SC [51]	88.4	96.1	-	-
Pyramid-Net [53]	88.2	95.7	98.4	99.0
ABDNet [7]	88.28	95.6	-	-
SONA [44]	88.8	95.58	98.5	99.18
TransReID [22] *	88.9	95.2	-	
ICC(ResNet50)	88.5	95.3	98.5	99.0
CCC(ResNet50)	87.1	95.3	98.4	99.0
DCC(ResNet50)	**89.2**	95.4	**98.5**	**99.2**
CLA(ResNet50-ibn) [6]	88.9	95.7	-	-
FastReID(ResNet50-ibn) [20]	89.3	95.7	-	-
ICC(ResNet50-ibn)	89.2	95.1	98.4	99.0
CCC(ResNet50-ibn)	88.4	95.3	98.1	99.0
DCC(ResNet50-ibn)	**89.8**	96.0	**98.8**	**99.2**

* The performance of the TransReID is the input size of 256×128, which is similar to our setting.

Table 3. Comparison of **Supervised** Person ReID on Market1501.

Firstly, we can observe that the proposed DCC is significantly better than existing methods with the same backbone, which proves the effectiveness of the proposed Dual Cluster Contrastive, *e.g.,* with the backbone of ResNet50-ibn, DCC obtains the mAP of 89.8%, and 64.9% for Market1501, and MSMT17, respectively. As shown in Table 4, the DCC obtains the worse performance than TransReID [22], *e.g.,* 64.9% vs 67.4%. The reason is that TransReID applies the transformer-based network as the backbone for person ReID, which is stronger than the ResNet used in DCC.

Secondly, based on whether considering the local features or additional information, existing methods can be divided into two groups: backbone-independent methods and feature-fusion methods. The feature-fusion methods propose the novel module to min multi-level discriminative clues for person ReID. The backbone-indpependent methods propose and add a backbone-indpependent modules on the backbone for inferring the discriminative description, *e.g.,* Contrastive Learning [13], Circle Loss [37], Triplet Loss, and Classification Loss. *Therefore, all backbone-independent methods use the same backbone for inferencing,* e.g., *ResNet50, or ResNet50-ibn, and making a comparison among them be a fair comparison.* Therefore, Dual Cluster Contrastive can be treated as a novel backbone-independent module. Compared with existing backbone-indpependent methods, we can observe that DCC obtains a noticeable improvement upon the existing methods, *e.g.,* improving the mAP from 87.4%, and 52.1% of Circle Loss [37] to 89.2%, and 60.6%. The superior performance demonstrates the effectiveness of the proposed DCC.

Methods	mAP	R1	R5	R10
MGN [39]+CircleLoss	52.1	76.9	-	-
Circle Loss [37]	52.1	76.9	-	-
DG-Net [56]	52.3	77.2	87.4	90.5
CAR [59]	52.9	78.7	-	-
CAL [36]	56.2	79.5	89.0	-
RGA-SC [51]	57.5	80.3	-	-
FastReID(ResNet50) [20]	59.9	83.3	-	-
ABDNet [7]	60.8	82.3	-	-
TransReID [22] *	**67.4**	**85.3**	-	
ICC(ResNet50)	57.2	80.0	89.2	91.7
CCC(ResNet50)	56.4	79.8	89.3	92.0
DCC(ResNet50)	60.6	82.5	90.7	93.1
FastReID(ResNet50-ibn) [20]	61.2	59.9	-	-
ICC(ResNet50-ibn)	61.9	83.2	91.2	93.4
CCC(ResNet50-ibn)	60.9	82.9	91.0	93.4
DCC(ResNet50-ibn)	64.9	85.1	**92.6**	**94.4**

* TransReID applies the Transformer as the backbone for person ReID, which is stronger than ResNet used in DCC.

Table 4. Comparison of **Supervised** Person ReID on MSMT17.

Finally, we evaluate the proposed DCC with different backbones to show its better generability. Since Instance normalization(IN) [38] and Batch normalization (BN) [25] can capture the appearance invariance and the content-related information, the Instance-batch normalization (IBN) [35] combining the advantage of the above-mentioned normalization has been proven to be effective for person ReID [20]. Therefore, by replacing the BN operation in ResNet50 with IBN operation, the ResNet50-ibn is treated as a strong backbone. From Table 3 and Table 4, we can observe that ResNet50-ibn obtain a higher performance than ResNet50, *e.g.,* compared with the ResNet50, using ResNet50-ibn improves the mAP from 89.2%, and 60.6% to 89.8%, and 64.9% for Market1501, and MSMT17, respectively.

Comparision on Unsupervised Person ReID In addition to the supervised person ReID, we further compare the Dual Cluster Contrastive with existing unsupervised person ReID methods and summarize the related results in Table 5, and Table 6. We can observe that DCC is significantly better than existing methods, which proves the effectiveness of the Dual Cluster Contrastive.

Disscussion The most related work to ours is the cluster contrastive. Compared with the vallina cluster contrastive, the Dual Cluster Contrastive has the following benefits based on the above analysis. Firstly, Dual Cluster Contrastive (DCC) is insensitive to the batch size. Secondly, DCC has a faster convergence speed during the training process. Thirdly, DCC has better generalization capabilities, *e.g.,* DCC achieves the better performance for both supervised and unsupervised person ReID on two datasets.

Methods	mAP	R1	R5	R10
SSG [16]	58.3	80.0	90.0	92.4
UGA [42]	70.3	87.2	-	-
NRMT [48]	71.7	87.8	94.6	96.5
JVTC+ [4]	75.4	90.5	96.2	97.1
MMT [17]	75.6	89.3	95.8	97.5
SPCL [18]	77.5	89.7	96.1	97.6
ICE [3]	79.2	92.0	97.0	98.1
GLT [54]	79.5	92.2	96.5	97.8
FastReID [20]	80.5	92.7	-	-
CACAL [30]	80.9	92.7	97.4	**98.5**
CC(ResNet50) [13]	82.6	93.0	97.0	98.1
CC(ResNet50-ibn) [13]	84.1	93.2	97.6	98.2
DCC(ResNet50)	83.8	93.4	97.1	98.2
DCC(ResNet50-ibn)	**84.7**	**93.8**	**97.4**	98.2

Table 5. Comparison of **Unsupervised** Person ReID on Market1501.

Methods	mAP	R1	R5	R10
ECN [16]	10.2	30.2	41.5	46.8
CACL [30]	21.0	45.4	55.6	63.6
UGA [42]	21.7	49.5	-	-
MMT [17]	24.0	50.1	63.5	69.3
SPCL [18]	26.8	53.7	65.0	69.8
FastReID [20]	27.7	59.5	-	-
JVTC+ [4]	29.7	54.4	68.2	74.2
ICE [3]	29.8	59.0	71.7	77.0
CC(ResNet50) [13]	33.3	63.3	73.7	77.8
CC(ResNet50-ibn) [13]	41.1	69.1	79.3	83.1
DCC(ResNet50)	34.3	65.0	75.2	79.1
DCC(ResNet50-ibn)	**41.8**	**71.0**	**80.5**	**83.8**

Table 6. Comparison of **Unsupervised** person ReID on MSMT17.

5. Conclusion

To overcome the limitation of the cluster contrastive for person ReID, we propose a novel Dual Cluster Contrastive framework, which consists of the individual-level cluster contrastive and centroid-level cluster contrastive. The individual-level cluster contrastive updates its memory bank based on the individual feature with the momentum update strategy, and the centroid-level cluster contrastive updates its memory bank with the mean feature of each class. The evaluations on two benchmarks under the supervised and unsupervised settings demonstrate the effectiveness of the proposed DCC.

Although the proposed Dual Cluster Contrative is a practical framework, it maintains two different memory banks, with certain limitations in applying a large-scale dataset. In the future, we will explore how to use one memory bank to achieve the benefits of the two memory banks through adaptive optimization strategies.

References

[1] Mathilde Caron, Ishan Misra, Julien Mairal, Priya Goyal, Piotr Bojanowski, and Armand Joulin. Unsupervised learning of visual features by contrasting cluster assignments. In Hugo Larochelle, Marc'Aurelio Ranzato, Raia Hadsell, Maria-Florina Balcan, and Hsuan-Tien Lin, editors, *NIPS*, 2020. 1

[2] Binghui Chen, Weihong Deng, and Jiani Hu. Mixed high-order attention network for person re-identification. In *ICCV*, pages 371–381, 2019. 1, 2, 7

[3] Hao Chen, Benoit Lagadec, and Francois Bremond. Ice: Inter-instance contrastive encoding for unsupervised person re-identification. *arXiv preprint arXiv:2103.16364*, 2021. 3, 8

[4] Hao Chen, Yaohui Wang, Benoit Lagadec, Antitza Dantcheva, and Francois Bremond. Joint generative and contrastive learning for unsupervised person re-identification. In *CVPR*, pages 2004–2013, 2021. 3, 8

[5] Peixian Chen, Wenfeng Liu, Pingyang Dai, Jianzhuang Liu, Qixiang Ye, Mingliang Xu, Qi'an Chen, and Rongrong Ji. Occlude them all: Occlusion-aware attention network for occluded person re-id. In *ICCV*, pages 11833–11842, October 2021. 1, 2

[6] Qiuyu Chen, Wei Zhang, and Jianping Fan. Cluster-level feature alignment for person re-identification. *CoRR*, abs/2008.06810, 2020. 7

[7] Tianlong Chen, Shaojin Ding, Jingyi Xie, Ye Yuan, Wuyang Chen, Yang Yang, Zhou Ren, and Zhangyang Wang. Abd-net: Attentive but diverse person re-identification. In *ICCV*, pages 8351–8361, 2019. 7, 8

[8] Ting Chen, Simon Kornblith, Mohammad Norouzi, and Geoffrey E. Hinton. A simple framework for contrastive learning of visual representations. In *ICML*, volume 119 of *PMLR*, pages 1597–1607. PMLR, 2020. 1

[9] Weihua Chen, Xiaotang Chen, Jianguo Zhang, and Kaiqi Huang. Beyond triplet loss: A deep quadruplet network for person re-identification. In *CVPR*, 2017. 1, 2

[10] Xinlei Chen and Kaiming He. Exploring simple siamese representation learning. In *CVPR*, pages 15750–15758. Computer Vision Foundation / IEEE, 2021. 1

[11] Yanbei Chen, Xiatian Zhu, and Shaogang Gong. Instance-guided context rendering for cross-domain person re-identification. In *ICCV*, 2019. 1, 3

[12] Yongxing Dai, Jun Liu, Yifan Sun, Zekun Tong, Chi Zhang, and Ling-Yu Duan. Idm: An intermediate domain module for domain adaptive person re-id. In *ICCV*, pages 11864–11874, 2021. 3

[13] Zuozhuo Dai, Guangyuan Wang, Weihao Yuan, Siyu Zhu, and Ping Tan. Cluster contrast for unsupervised person re-identification. *arXiv preprint arXiv:2103.11568*, 2021. 1, 3, 4, 5, 6, 7, 8

[14] Jia Deng, Wei Dong, Richard Socher, Li-Jia Li, Kai Li, and Li Fei-Fei. Imagenet: A large-scale hierarchical image database. In *CVPR*, pages 248–255. Ieee, 2009. 5

[15] Guodong Ding, Salman Khan, and Zhenmin Tang. Dispersion based clustering for unsupervised person re-identification. In *BMVC*, 2019. 3

[16] Yang Fu, Yunchao Wei, Guanshuo Wang, Yuqian Zhou, Honghui Shi, and Thomas S Huang. Self-similarity grouping: A simple unsupervised cross domain adaptation approach for person re-identification. In *ICCV*, pages 6112–6121, 2019. 1, 2, 3, 8

[17] Yixiao Ge, Dapeng Chen, and Hongsheng Li. Mutual mean-teaching: Pseudo label refinery for unsupervised domain adaptation on person re-identification. *arXiv preprint arXiv:2001.01526*, 2020. 1, 3, 8

[18] Yixiao Ge, Feng Zhu, Dapeng Chen, Rui Zhao, and Hongsheng Li. Self-paced contrastive learning with hybrid memory for domain adaptive object re-id. In Hugo Larochelle, Marc'Aurelio Ranzato, Raia Hadsell, Maria-Florina Balcan, and Hsuan-Tien Lin, editors, *NeurIPS*, 2020. 1, 3, 8

[19] Kaiming He, Xiangyu Zhang, Shaoqing Ren, and Jian Sun. Deep residual learning for image recognition. In *CVPR*, pages 770–778, 2016. 5

[20] Lingxiao He, Xingyu Liao, Wu Liu, Xinchen Liu, Peng Cheng, and Tao Mei. Fastreid: A pytorch toolbox for general instance re-identification. *arXiv preprint arXiv:2006.02631*, 2020. 7, 8

[21] Shuting He, Hao Luo, Pichao Wang, Fan Wang, Hao Li, and Wei Jiang. Transreid: Transformer-based object re-identification. In *ICCV*, pages 15013–15022, October 2021. 2

[22] Shuting He, Hao Luo, Pichao Wang, Fan Wang, Hao Li, and Wei Jiang. Transreid: Transformer-based object re-identification. *CoRR*, abs/2102.04378, 2021. 7, 8

[23] Alexander Hermans, Lucas Beyer, and Bastian Leibe. In defense of the triplet loss for person re-identification. *CoRR*, abs/1703.07737, 2017. 1, 2

[24] Yangru Huang, Peixi Peng, Yi Jin, Yidong Li, and Junliang Xing. Domain adaptive attention learning for unsupervised person re-identification. In *AAAI*, pages 11069–11076, Apr. 2020. 3

[25] Sergey Ioffe and Christian Szegedy. Batch normalization: Accelerating deep network training by reducing internal covariate shift. In Francis R. Bach and David M. Blei, editors, *ICML*, volume 37 of *JMLR Workshop and Conference Proceedings*, pages 448–456. JMLR.org, 2015. 6, 8

[26] Takashi Isobe, Dong Li, Lu Tian, Weihua Chen, Yi Shan, and Shengjin Wang. Towards discriminative representation learning for unsupervised person re-identification. In *ICCV*, pages 8526–8536, 2021. 3

[27] Mahdi M Kalayeh, Emrah Basaran, Muhittin Gökmen, Mustafa E Kamasak, and Mubarak Shah. Human semantic parsing for person re-identification. In *CVPR*, pages 1062–1071, 2018. 2

[28] Shenqi Lai, Zhenhua Chai, and Xiaolin Wei. Transformer meets part model: Adaptive part division for person re-identification. In *ICCV Workshops*, pages 4150–4157, October 2021. 2

[29] Jianing Li, Shiliang Zhang, Qi Tian, Meng Wang, and Wen Gao. Pose-guided representation learning for person re-identification. *IEEE TPAMI*, 2019. 2

[30] Mingkun Li, Chun-Guang Li, and Jun Guo. Cluster-guided asymmetric contrastive learning for unsupervised person re-

identification. *arXiv preprint arXiv:2106.07846*, 2021. 1, 3, 8

[31] Yutian Lin, Xuanyi Dong, Liang Zheng, Yan Yan, and Yi Yang. A bottom-up clustering approach to unsupervised person re-identification. In *AAAI*, 2019. 3

[32] Jiawei Liu, Zheng-Jun Zha, Di Chen, Richang Hong, and Meng Wang. Adaptive transfer network for cross-domain person re-identification. In *CVPR*, 2019. 1, 3

[33] Xiaobin Liu and Shiliang Zhang. Domain adaptive person re-identification via coupling optimization. In *ACM MM*, pages 547–555, 2020. 3

[34] Hao Luo, Youzhi Gu, Xingyu Liao, Shenqi Lai, and Wei Jiang. Bag of tricks and a strong baseline for deep person re-identification. In *CVPR Workshops*, pages 1487–1495. Computer Vision Foundation / IEEE, 2019. 6

[35] Xingang Pan, Ping Luo, Jianping Shi, and Xiaoou Tang. Two at once: Enhancing learning and generalization capacities via ibn-net. In *ECCV*, volume 11208 of *Lecture Notes in Computer Science*, pages 484–500. Springer, 2018. 8

[36] Yongming Rao, Guangyi Chen, Jiwen Lu, and Jie Zhou. Counterfactual attention learning for fine-grained visual categorization and re-identification. *CoRR*, abs/2108.08728, 2021. 7, 8

[37] Yifan Sun, Changmao Cheng, Yuhan Zhang, Chi Zhang, Liang Zheng, Zhongdao Wang, and Yichen Wei. Circle loss: A unified perspective of pair similarity optimization. In *CVPR*, pages 6398–6407, 2020. 7, 8

[38] Dmitry Ulyanov, Andrea Vedaldi, and Victor S. Lempitsky. Improved texture networks: Maximizing quality and diversity in feed-forward stylization and texture synthesis. In *CVPR*, pages 4105–4113. IEEE Computer Society, 2017. 8

[39] Guanshuo Wang, Yufeng Yuan, Xiong Chen, Jiwei Li, and Xi Zhou. Learning discriminative features with multiple granularities for person re-identification. In *ACM MM*, pages 274–282, 2018. 7, 8

[40] Longhui Wei, Shiliang Zhang, Wen Gao, and Qi Tian. Person transfer gan to bridge domain gap for person re-identification. In *CVPR*, pages 79–88, 2018. 3, 5

[41] Nicolai Wojke and Alex Bewley. Deep cosine metric learning for person re-identification. In *WACV*, pages 748–756. IEEE, 2018. 3

[42] Jinlin Wu, Yang Yang, Hao Liu, Shengcai Liao, Zhen Lei, and Stan Z Li. Unsupervised graph association for person re-identification. In *ICCV*, pages 8321–8330, 2019. 8

[43] Zhirong Wu, Yuanjun Xiong, Stella X. Yu, and Dahua Lin. Unsupervised feature learning via non-parametric instance discrimination. In *CVPR*, pages 3733–3742. Computer Vision Foundation / IEEE Computer Society, 2018. 4

[44] Bryan Ning Xia, Yuan Gong, Yizhe Zhang, and Christian Poellabauer. Second-order non-local attention networks for person re-identification. In *ICCV*, pages 3760–3769, 2019. 1, 2, 7

[45] Tong Xiao, Shuang Li, Bochao Wang, Liang Lin, and Xiaogang Wang. Joint detection and identification feature learning for person search. In *CVPR*, pages 3376–3385. IEEE Computer Society, 2017. 1, 3

[46] Hong-Xing Yu, Wei-Shi Zheng, Ancong Wu, Xiaowei Guo, Shaogang Gong, and Jian-Huang Lai. Unsupervised person re-identification by soft multilabel learning. In *CVPR*, 2019. 3

[47] Kaiwei Zeng, Munan Ning, Yaohua Wang, and Yang Guo. Hierarchical clustering with hard-batch triplet loss for person re-identification. In *CVPR*, pages 13657–13665, 2020. 3

[48] Yunpeng Zhai, Qixiang Ye, Shijian Lu, Mengxi Jia, Rongrong Ji, and Yonghong Tian. Multiple expert brainstorming for domain adaptive person re-identification. In *ECCV*, pages 594–611. Springer, 2020. 3, 8

[49] Xinyu Zhang, Jiewei Cao, Chunhua Shen, and Mingyu You. Self-training with progressive augmentation for unsupervised cross-domain person re-identification. In *ICCV*, 2019. 1, 3

[50] Zhizheng Zhang, Cuiling Lan, Wenjun Zeng, Xin Jin, and Zhibo Chen. Relation-aware global attention for person re-identification. In *CVPR*, June 2020. 1, 2

[51] Zhizheng Zhang, Cuiling Lan, Wenjun Zeng, Xin Jin, and Zhibo Chen. Relation-aware global attention for person re-identification. In *CVPR*, pages 3183–3192. Computer Vision Foundation / IEEE, 2020. 7, 8

[52] Zhong Zhang, Haijia Zhang, and Shuang Liu. Person re-identification using heterogeneous local graph attention networks. In *CVPR*, pages 12136–12145, 2021. 1, 2

[53] Feng Zheng, Cheng Deng, Xing Sun, Xinyang Jiang, Xiaowei Guo, Zongqiao Yu, Feiyue Huang, and Rongrong Ji. Pyramidal person re-identification via multi-loss dynamic training. In *CVPR*, pages 8514–8522, 2019. 2, 7

[54] Kecheng Zheng, Wu Liu, Lingxiao He, Tao Mei, Jiebo Luo, and Zheng-Jun Zha. Group-aware label transfer for domain adaptive person re-identification. In *CVPR*, pages 5310–5319, 2021. 3, 8

[55] Liang Zheng, Liyue Shen, Lu Tian, Shengjin Wang, Jingdong Wang, and Qi Tian. Scalable person re-identification: A benchmark. In *ICCV*, pages 1116–1124, 2015. 5

[56] Zhedong Zheng, Xiaodong Yang, Zhiding Yu, Liang Zheng, Yi Yang, and Jan Kautz. Joint discriminative and generative learning for person re-identification. In *CVPR*, pages 2138–2147, 2019. 8

[57] Zhun Zhong, Liang Zheng, Shaozi Li, and Yi Yang. Generalizing a person retrieval model hetero-and homogeneously. In *ECCV*, 2018. 1, 3

[58] Zhun Zhong, Liang Zheng, Zhiming Luo, Shaozi Li, and Yi Yang. Invariance matters: Exemplar memory for domain adaptive person re-identification. In *CVPR*, 2019. 3

[59] Kaiyang Zhou, Yongxin Yang, Andrea Cavallaro, and Tao Xiang. Omni-scale feature learning for person re-identification. In *ICCV*, pages 3702–3712, 2019. 7, 8

[60] Sanping Zhou, Jinjun Wang, Rui Shi, Qiqi Hou, Yihong Gong, and Nanning Zheng. Large margin learning in set-to-set similarity comparison for person reidentification. *IEEE TMM*, 20(3):593–604, 2017. 1, 2

[61] Sanping Zhou, Jinjun Wang, Jiayun Wang, Yihong Gong, and Nanning Zheng. Point to set similarity based deep feature learning for person re-identification. In *CVPR*, 2017. 2